Automation and Machine Learning (2024)
Clausius Scientific Press, Canada

DOI: 10.23977/autml.2024.050102
ISSN 2516-5003 Vol. 5 Num. 1

Control Method of Temperature for Multi-stack Fuel Cell System

Zhou Su[1,a], Yang Ning[1,b,*], Chen Chunguang[1,c]

[1]College of Automotive Studies, Tongji University, Shanghai, 201804, China
[a]suzhou@tongji.edu.cn, [b]2131588@tongji.edu.cn, [c]2031636@tongji.edu.cn
[*]Corresponding author

Keywords: Multi-stack fuel cell system, thermal management subsystem, model predictive control, BP neural network, dynamic matrix control

Abstract: In order to control each stack temperature in a multi-stack fuel cell system (MFCS), a model prediction control algorithm based on back propagation neural network (BPNN) is proposed. Firstly, a parallel multi-stack fuel cell thermal management subsystem model was established and a BP neural network system prediction model was trained by applying the system model simulation data; then, the step response matrix of the system prediction model was obtained at typical operating conditions and a dynamic matrix controller was designed; finally, a test operating condition was designed for simulation analysis. The results show that the dynamic matrix controller (DCM) based on BPNN can quickly and accurately control the temperature of the multi-stack fuel cell system, while having the characteristics of small overshoot and short regulation time.

1. Introduction

As an energy conversion device, proton exchange membrane fuel cell (PEMFC) is widely regarded as one of the alternatives to traditional vehicle power sources for its low operating temperature, high specific energy, and fast start-up speed [1]. However, the power of PEMFC with single stack cannot meet the demands of diverse operating conditions and high-power application scenarios [2], and its structural limitations make the system less fault-tolerant. In order to solve the above problems, Multi-stack Fuel Cell System has emerged. The parallel use of multiple stacks can not only improve the power of the system, but also enhance the fault tolerance and reliability of the system [3]. In addition, the introduction of multiple stacks makes the optimal allocation of power possible, thus contributing to the overall system efficiency [4].

Most of the automotive fuel cells are PEMFCs, in which the membranes are prone to decomposition at high temperatures. Therefore, the internal temperature of PEMFC needs to be kept within a reasonable range (60~90 ℃). The regions of the fuel cell involving electrochemical reactions need to maintain suitable temperature, which have an important impact on the fuel cell electrochemical reaction rate, reaction gas pressure, and remaining useful life (RUL) [5,6]. Therefore, timely and stable thermal management is very important for the safety and performance guarantee of fuel cells. Experts at home and abroad have carried out a lot of research work on temperature control of PEMFC. O'Keefe et al [7] designed a time-varying PI controller for a 5kW water-cooled

fuel cell system to control the cell temperature by the flow rate of the cooling water, and the results demonstrated the good performance of the proposed control method. Pei Yaowang et al [8] proposed a controller based on an adaptive linear quadratic regulator and experimentally verified that the controller has good control performance. Arce et al [9] designed a Model Predictive controller (MPC) for the thermal management subsystem with the target of maximising the efficiency and minimising the RUL of the fuel cell, which obtained good control results. Shen Wei et al [10] used a system identification approach to establish linear predictive models in different steady-state operating conditions points of MFCS thermal management subsystem and designed a MPC controller. The results show that it can quickly and accurately perform the temperature control of each stack in the MFCS. Zhao Hongbo et al [11] designed a neural network-based self-resistant controller, replacing the nonlinear error feedback control law with a neural network model, and their simulation verified that the controller has a better control quality under the disturbances of different degrees of noise.

In this paper, a parallel MFCS thermal management subsystem, which consists of three stacks with rated power of 20kW, 70kW and 120kW respectively, is designed with reference to the single-stack PEMFC system model and temperature control method. According to the dynamic analysis of heat balance, the MPC algorithm is used to control the temperature of each stack with large time lag in real time. Firstly, a back propagation neural network (BPNN) is applied to establish a prediction model for the thermal management subsystem of MFCS. Secondly, the step response matrix of the system prediction model is obtained through the principle of linear superposition at typical working conditions. Then a Dynamic Matrix Controller (DMC) is designed to control the temperature of MFCS. Finally, the performance of controller is verified under given operating condition.

2. Model of MFCS Thermal Management Subsystem

Based on the power requirement of a heavy commercial vehicle, a set of MFCS with a total power of 210 kW is matched. According to [12], when the power of each stack is optimally allocated using the RUL and efficiency as the comprehensive optimization indexes, the optimal split-stack scheme is three stacks with the rated power of 20 kW, 70 kW, and 120 kW, respectively. In this paper, a related work is carried out on the basis of the MFCS established by this method.

2.1. Architecture of Proposed Thermal Management Subsystem

The design of the MFCS thermal management subsystem structure not only needs to meet the heat dissipation requirements of different components, but also to ensure the functional independence of the thermal management subsystem. The temperature control mode of MFCS mainly based on water cooling. The thermal management subsystem of MFCS is designed on the basis of the single-stack fuel cell structure [13], and its structure is shown in Figure. 1.

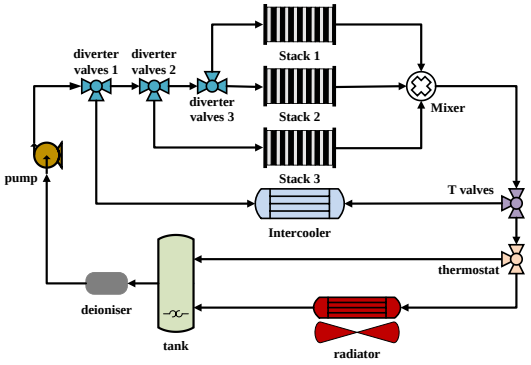

Figure 1: Architecture of proposed thermal management subsystem.

2.2. Modelling of Proposed Thermal Management Subsystem

Assuming that the heat flow is the same for the three stacks, the heat exchange process of the stacks is analysed using a single stack as an example. The heat balance relationship of the stack is mainly divided into internal electrochemical reaction heat generation and heat transfer with the outside world [14]. The heat balance expression of the stack is given by

$$\dot{Q}_{cg} = \dot{Q}_{react} + \dot{Q}_{an} + \dot{Q}_{ca} + \dot{Q}_{cool} - \dot{Q}_{\mathrm{rad}} - \dot{Q}_{\mathrm{conv}} \tag{1}$$

where $\dot{Q}_{cg}$ is exchange heat of stack in kW, $\dot{Q}_{react}$ is the heat produced from the reaction inside the stack, $\dot{Q}_{an}$ is the difference between the heat carried by reactants of anode inlet and outlet, $\dot{Q}_{ca}$ is the difference between the heat carried by reactants of cathode inlet and outlet, $\dot{Q}_{cool}$ is the heat removed from the cell by coolant, $\dot{Q}_{\mathrm{rad}}$ is heat radiation, $\dot{Q}_{\mathrm{conv}}$ is heat convection.

The heat production from the electrochemical reactions inside stack can be described as

$$\dot{Q}_{react} = I_{st}(nE_{the} - V_{st}) \tag{2}$$

where I_{st} is the current of stack in A, n is the number of cells in stack , E_{the} is theoretical maximum electric potential of a cell in V, V_{st} output voltage of stack in V.

The heat exchange between the fuel cell stack and the outside world mainly includes the heat exchange with the reactants, coolant and environment. The heat exchange with the reactants can be obtained by the difference between the heat carried by the imported and exported substances which are modelled by

$$\dot{Q}_{an} = \dot{Q}_{an,in}^{H_2} + \dot{Q}_{an,in}^{vap} - \dot{Q}_{an,out}^{H_2} - \dot{Q}_{an,out}^{vap} - \dot{Q}_{an,out}^{liq} \tag{3}$$

$$\dot{Q}_{ca} = \dot{Q}_{ca,in}^{O_2} + \dot{Q}_{ca,in}^{N_2} + \dot{Q}_{ca,in}^{vap} - \dot{Q}_{ca,out}^{O_2} - \dot{Q}_{ca,out}^{N_2} - \dot{Q}_{ca,out}^{vap} - \dot{Q}_{ca,out}^{liq} \tag{4}$$

where the superscript H_2, vap, O_2, N_2, liq are hydrogen, oxygen, nitrogen, vapour and liquid water, respectively, the subscripts ca, an, in and out are cathode, anode, inlet and outlet.

The heat exchange between the stack and the coolant can be obtained from the difference between the heat carried by the coolant in the stack's inlet and outlet, and be described as

$$\dot{Q}_{cool} = \dot{m}c_p(T_{cool,in} - T_{cool,out}) \tag{5}$$

where $\dot{m}$ is water mass flow rate trough the cell in kg/s, c_p is heat capacity of coolant in $\mathrm{J/(kg \cdot K)}$, $T_{cool,in}$ and $T_{cool,out}$ are the inlet and outlet water temperature in K, respectively.

Heat convection and radiation are two main types of heat exchange between stack and the environment, which are given by

$$\dot{Q}_{conv} = hA_{conv}(T_{st} - T_0) \tag{6}$$

$$\dot{Q}_{rad} = \varepsilon\sigma A_{rad}(T_{st}^4 - T_0^4) \tag{7}$$

where h is the convection heat transfer coefficient in $\mathrm{W/(m^2 \cdot K)}$, A_{conv} is the effective contact area of heat convection in $\mathrm{m^2}$, T_{st} is the temperature of stack in K, T_0 is ambient temperature in K, ε is the emissivity of stack, σ is Stefan-Boltzmann constant , A_{rad} is the effective contact area of heat radiation in $\mathrm{m^2}$.

3. Proposed Temperature Control Algorithm of MFCS

The MPC algorithm is good at handling system with problems of multivariate and large time lag. It is a method with excellent performance for the MFCS temperature control problem [15]. Therefore, the MPC algorithm is selected to control the system temperature in order to obtain better control results.

3.1. Architecture of MFCS Control Algorithm

In this paper, the radiator, coolant circulation pump, diverter valve 2 and diverter valve 3 are selected as actuators. The current of each stack is treated as a disturbance input to the system, and the structure of the established MPC controller is shown in Figure.2. The reference temperature of all three stacks is set to 75 ℃, and the coolant inlet reference temperature is set to 65 ℃. Mapping relationship of input and output is shown as

$$\begin{bmatrix} n_{\text{pump}} \\ n_{\text{fan}} \\ \varphi_2 \\ \varphi_3 \end{bmatrix} \rightarrow \begin{bmatrix} T_{\text{st},1} \\ T_{\text{st},2} \\ T_{\text{st},3} \\ T_{\text{st,in}} \end{bmatrix} \tag{8}$$

where n_{pump} is the speed of pump in rpm, n_{fan} is the speed of radiator fans in rpm, φ_2 is the opening of diverter valve 2, φ_3 is the opening of diverter valve 3, $T_{\text{st},1}$, $T_{\text{st},2}$, $T_{\text{st},3}$ and $T_{\text{st,in}}$ are the temperature of stack 1,stack 2, stack 3 and coolant.

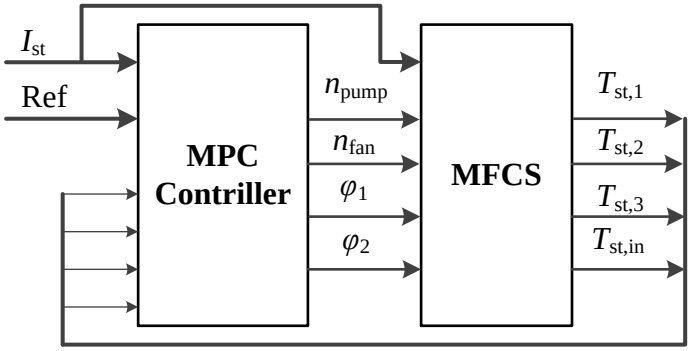

Figure 2: MPC controller architecture of MFCS thermal management subsystem.

3.2. BPNN Prediction Model of MFCS Thermal Management Subsystem

BPNN is a multi-layer feed-forward neural network based on artificial neuron model, and the parameters in the neural network are trained by back-propagation algorithm [16]. The BPNN has a good fitting ability for nonlinear system, thus it is possible to train a BPNN as a nonlinear prediction model for the thermal management subsystem of the MFCS to reflect the temperature change characteristics under different operating conditions.

The nonlinear system prediction model can be represented by

$$y(k+1) = f(u(k-m),...,u(k-1),u(k),y(k-n),...,y(k-1),y(k)) \tag{9}$$

where $u(k)$ and $y(k)$ are system inputs and outputs at the time of k, m and n are the index of the inputs and outputs of the system respectively.

The inputs of the thermal management subsystem at the moment of (k-1) and the inputs and outputs at the moment of k are selected as inputs to the BPNN, and the outputs of the system at the (k+1) moment are used as desired outputs to train the neural network. Define the input and output of the system as shown in equation

$$u=\begin{bmatrix} n_{\text{pump}} \\ n_{\text{fan}} \\ \varphi_2 \\ \varphi_3 \\ I_{\text{st,1}} \\ I_{\text{st,2}} \\ I_{\text{st,3}} \end{bmatrix}, y=\begin{bmatrix} T_{\text{st,1}} \\ T_{\text{st,2}} \\ T_{\text{st,3}} \\ T_{\text{st,in}} \end{bmatrix} \tag{10}$$

where $I_{\text{st,1}}$, $I_{\text{st,2}}$ and $I_{\text{st,3}}$ are current of each stack.

A random signal is applied to the system based on the relationship between input and output to obtain the output of the system. The input and output data of the system are paired to form the original training data, and the BPNN is trained by MATLAB toolbox. The structure and parameters of the established neural network are shown in Table 1.

Table 1: The parameter of BPNN.

Parameter	Layer architecture	Activation function	Epoch
Value	18×13×4	Sigmoid	302

The accuracy of the trained BPNN prediction model is examined by designing the validation working condition, and the validation results are shown in Figure. 3. It can be seen that the maximum error between the BPNN outputs of the three stacks and the temperature of the inlet coolant and the actual data of the system is only ±0.2 ℃, which indicates that the single-step prediction model is able to accurately describe the dynamic characteristics of the system.

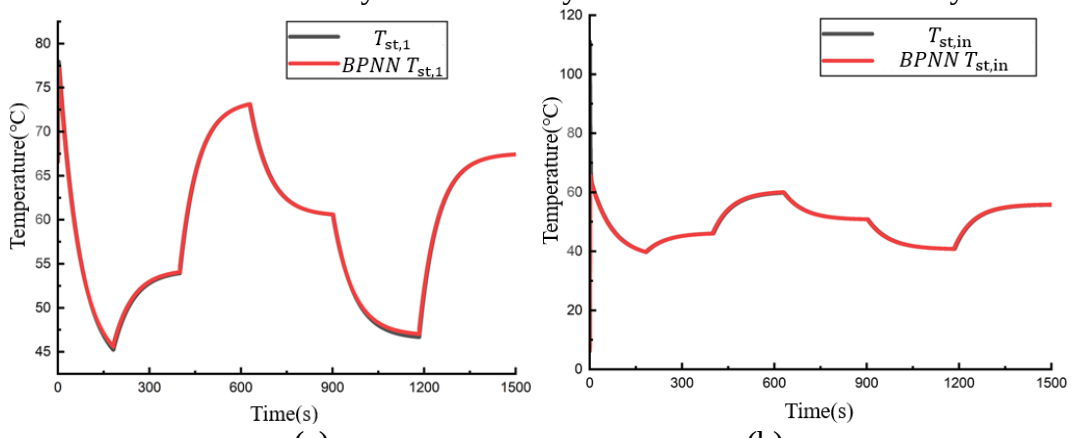

(a) (b)

Figure 3: BPNN prediction model validation of (a) stack 1 and (b) inlet coolant.

while designing the MPC controller it is necessary to obtain the system prediction response over the entire prediction horizon p. A p-step prediction of the system can be made as shown as

$$y(k+p)=f(u(k+p-m),\ldots,u(k+p-1),y(k+p-n),\ldots,y(k+p-1)) \tag{11}$$

Multiple single-step prediction neural network models are connected in series to form a recursive prediction network to satisfy the MPC requirements for performance prediction in the prediction horizon. The recursive neural network prediction model is shown in Figure. 4, which predicts the

system response at each sampling moment, and then builds the MPC controller by predicting the system response in the prediction horizon. At the same time, the feedback correction function in the MPC is realised based on the difference between the output of the prediction model and the output of the actual system at the current sampling moment as the feedback correction quantity.

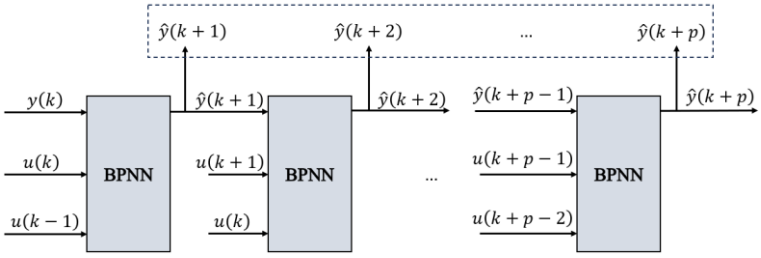

Figure 4: Recursive multi-step BPNN prediction model.

3.3. Design of DCM Controller

A typical method in MPC algorithm is DMC, which is based on the principle of model prediction by means of a unit step response model of the system, and the control law of the system is obtained by solving the optimisation problem [17]. Due to the output of the system after prediction by BPNN has nonlinearity, it is assumed that the system satisfies the linear superposition principle when the step response model is obtained.

Considering the n-dimensional measurable disturbances *d*, the unit step response model of the multiple-input multiple-output system is shown as

$$Y(k) = M_{ss}Y(k-1) + S_u\Delta u(k-1) + S_d\Delta d(k-1) \tag{12}$$

where M_{ss} is the state transfer matrix, S_u and S_d are the input matrix and measurable disturbance matrix of the unit step response state space model, respectively.

According to the basic principle of predictive control, assuming that the control horizon is *m* and the prediction horizon is *p*. Firstly, a *p*-step prediction is made based on Eq. (12), and the output sequence of the system in the prediction horizon can be expressed as

$$Y_p(k+1|k) = MY(k) + \hat{S}_u\Delta U(k) + \hat{S}_d\Delta d(k) \tag{13}$$

where $Y_p(k+1|k)$ is the output sequence within the prediction horizon *p*, $\Delta U(k)$ is the control sequence within the control horizon *m*, M, $\hat{S}_u$ and $\hat{S}_d$ are the state transfer matrix, input matrix, and measurable disturbance matrix in the prediction horizon, respectively.

Considering the input and output constraints of the system, the optimal quadratic control performance indicator can be expressed as

$$J = \left\|\Gamma_y(Y_p(k+1|k) - R(k+1))\right\|^2 + \left\|\Gamma_u\Delta U(k)\right\|^2 \tag{14}$$

where Γ_y is error weighting matrix, Γ_u is control weighting matrix, $R(k+1|k)$ is the sequence of reference values in the prediction horizon *p*.

Quadratic Programming is used to solve the solution of the optimisation problem. $\Delta U(k)$ is extracted as the optimisation variable and transformed into the quadratic programming standard form as shown as

$$J = \Delta U(k)^T H\Delta U(k) - G(k+1|k)^T\Delta U(k) \tag{15}$$

$$H = \hat{S}_u^T \Gamma_y^T \Gamma_y \hat{S}_u + \Gamma_u^T \Gamma_u$$
$$G(k+1|k) = 2\hat{S}_u^T \Gamma_y^T \Gamma_y E_p(k+1|k) \tag{16}$$
$$E_p(k+1|k) = R(k+1) - M_{ss} Y(k) - S_d \Delta d(k)$$

where $E_p(k+1|k)$ is the error between the desired output and the predicted output of the system.

The optimisation sequence $\Delta U(k)$ is obtained by the quadratic programming algorithm, taking the first control increment $\Delta u(k)$ of the optimisation sequence. Based on the control quantity $u(k-1)$ of the previous moment and the control increment of the current moment $\Delta u(k)$, the current control quantity $u(k)$ is calculated and applied to the controlled system. Then the control quantity of the system at the next moment is calculated according to the mechanism of "rolling time domain and repeating" in MPC theory.

The constraints of the system need to be taken into account when designing the controller. For the system, the input and output constraints are set as shown in Table 2. Considering the hysteresis of the temperature change of the MFCS, the prediction time domain p is selected as 40, the control time domain m is 10, and the sampling time is 1s. The system is designed to be robust to the temperature change of the MFCS.

Table 2: The constraints of MPC controller.

Parameter	Min Value	Max Value	Constraint Type
n_{pump}	50	4500	hard
n_{fan}	50	5000	hard
φ_2	0.1	0.95	hard
φ_3	0.1	0.95	hard
$T_{st,1}$	313.15	363.15	soft
$T_{st,2}$	313.15	363.15	soft
$T_{st,3}$	313.15	363.15	soft
$T_{st,in}$	313.15	363.15	soft

4. Validation of the DCM Controller

4.1. Design of Validation Condition

The traditional verification conditions are mainly step conditions, but the ideal step conditions do not exist in the actual system. In order to verify the effect of the proposed controller, step-like conditions are used instead of standard step conditions. The designed switching slope is 2A/s, and the operating current range of the stack is between 0 and 300 A. Seven switching points are set in the operating current range to validate the controller, and the validation conditions are shown in Figure. 5.

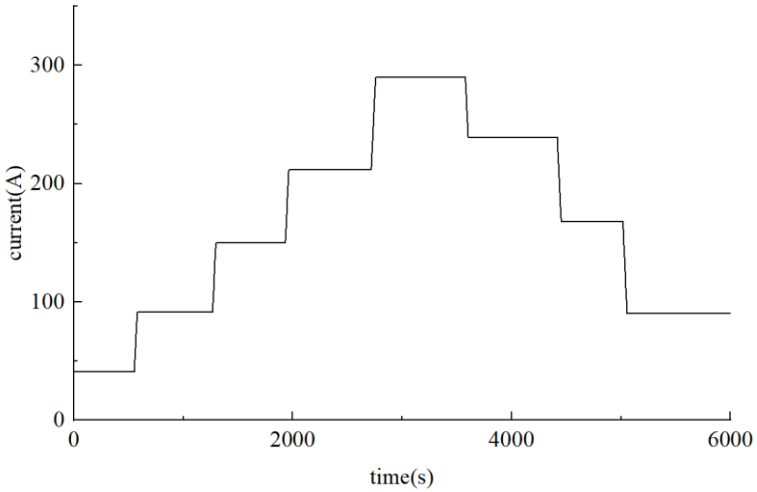

Figure 5: Validation conditions.

4.2. Results and discussions of the proposed controller

The MPC controller based on the piecewise linearization is a classical method for the temperature control of the MFCS [10]. The performance of two control methods, MPC based on piecewise linearization and DCM based on BPNN, are compared and analysed through simulation. Firstly, the step response matrix and state space model corresponding to the steady state points of the system at 60 A, 140 A and 240 A need to be obtained under offline conditions, respectively. Then, the step response matrix and state space model are switched according to the current magnitude of the three power stacks. The switching rules are shown in Table 3.

Table 3: Switching Rules of Predictive Model.

Steady State Points(A)	Current range(A)
60	0~100
140	100~200
240	200~300

The above two controller are used to control the temperature of the MFCS. Some output results of the two controllers are plotted in Figure. 6 and Figure. 7. It can be seen that compared with the MPC controller based on piecewise linearization, the speed of pump and fan controlled by DMC controller based on the BPNN is much smoother and so are the openings of diverter valves 2 and 3, and there is no violent fluctuation at the switching point of the operating conditions.

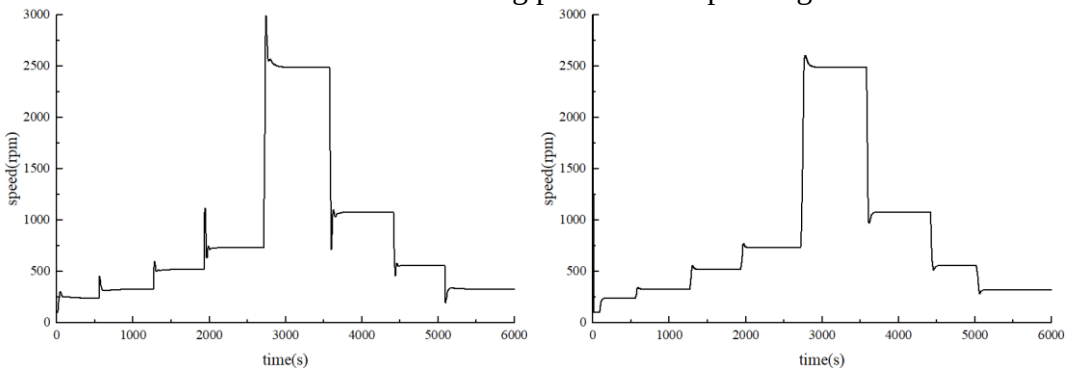

Figure 6: The speed of radiator fan with (a) linear based MPC and (b) BPNN based DCM.

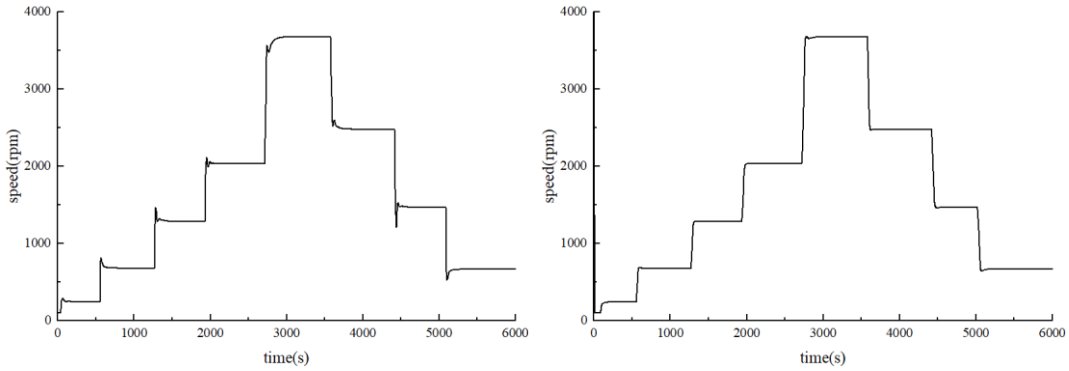

Figure 7: The speed of pump with (a) linear based MPC and (b) BPNN based DCM.

The simulation results of temperature controlled by the above two methods are shown in Fig. 8, from which we make the following observations.

(1) Under the control of MPC based on piecewise linearization, the maximum overshoot of the temperature is more than 3 ℃, and it takes 280 s for the temperature to return to stability when the operating condition changes.

(2) Under the control of DCM based on BPNN, the maximum error between the simulated and the ideal temperature can be maintained within 1.5 ℃, and the temperature can be adjusted to the ideal temperature smoothly and robustly within 180 s when the operating condition changes.

(3) The simulation results show that the designed DMC has a good control effect compared with MPC based on piecewise linearization.

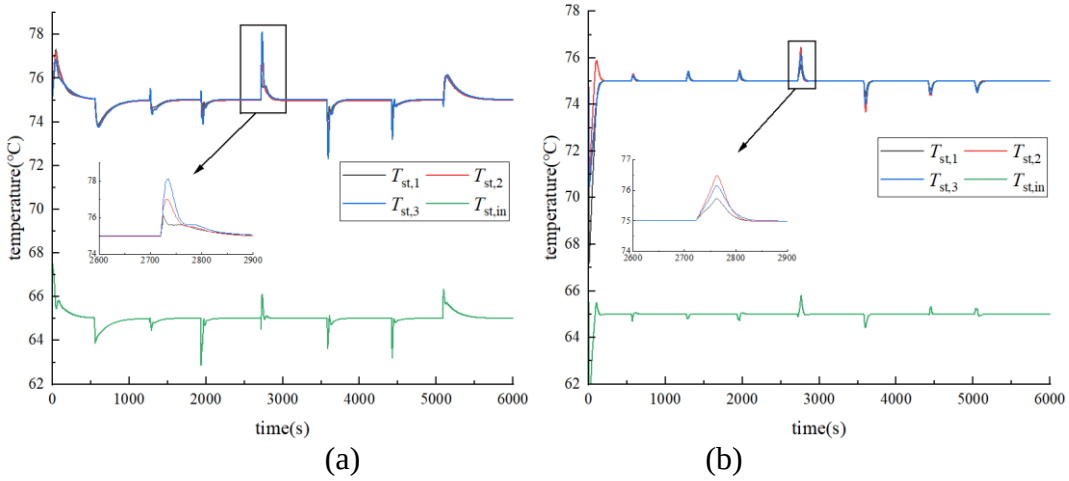

Figure 8: The simulation results of (a) linear based MPC and (b) BPNN based DCM.

5. Conclusions

A thermal management subsystem model of the parallel MFCS is built, and a BPNN-based DMC is designed to control the MFCS temperature. Replacing the linear prediction model with the BPNN can better deal with the mismatch between the prediction model and the real system in MPC, which greatly improves the accuracy of prediction model and the performance of the controller. The step-like conditions are used to validate the performance of the BPNN based DCM compared to linear based MPC. The results show that the fluctuation of the MFCS temperature is maintained within 1.5 ℃ and the temperature regulation time is within 180s, which indicates that the performance of proposed DCM is obviously better than that linear based MPC. In conclusion, the BPNN based

DMC with is robust and more suitable for the control of MFCS temperature, which has certain application value.

References

[1] Mat Z B A, Kar Y B, Hassan S H B A, et al. Proton exchange membrane (PEM) and solid oxide (SOFC) fuel cell based vehicles-a review[C]. 2017 2nd IEEE international conference on intelligent transportation engineering (ICITE). IEEE, 2017: 123-126.

[2] Forrest K, Mac Kinnon M, Tarroja B, et al. Estimating the technical feasibility of fuel cell and battery electric vehicles for the medium and heavy duty sectors in California[J]. Applied Energy, 2020, 276: 115439.

[3] Marx N, Cardozo J, Boulon L, et al. Comparison of the series and parallel architectures for hybrid multi-stack fuel cell-battery systems[C]. 2015 IEEE vehicle power and propulsion conference (VPPC). IEEE, 2015: 1-6.

[4] Zhou Su, Fan Lei, Zhang Gang, et al. A review on proton exchange membrane multi-stack fuel cell systems: Architecture, performance, and power management[J]. Applied Energy, 2022, 310: 118555.

[5] Zhang Guobin, Jiao Kui. Multi-phase models for water and thermal management of proton exchange membrane fuel cell: A review [J]. Journal of Power Sources, 2018, 391(JUL.1): 120-133.

[6] Gao Jianhua, Liu Yongfeng, Pei Pucheng, et al. An analysis of the temperature fluctuation effect on proton exchange membrane fuel cell[J]. Renewable Energy Resources, 2017, 35(8):6.(in Chinese)

[7] O'keefe D, El-Sharkh M Y, Telotte J C, et al. Temperature dynamics and control of a water-cooled fuel cell stack[J]. Journal of Power Sources, 2014, 256: 470-478.

[8] Pei Yaowang, Chen Fengxiang, Hu Zhe, et al. Temperature control of proton exchange membrane fuel cell thermal management system based on adaptive LQR control[J]. Journal of Jilin University (Engineering and Technology Edition), 2022, 52(09):2014-2024. (in Chinese)

[9] Arce A, Panos C, Bordons C, et al. Design and Experimental Validation of an Explicit MPC Controller for Regulating Temperature in PEM Fuel Cell Systems[J]. IFAC Proceedings Volumes, 2011, 44(1): 2476-2481.

[10] Shen Wei, Shi Lin, Chen Chunguang, et al. Analysis of Temperature Model Predictive Control of a Multi-Stack Fuel Cell System[J]. Journal of Tongji University (Natural Science), 2022, 50(09): 1368-1376. (in Chinese)

[11] Zhao Hongbo, Liu Jie, Ma Biao, et al. Control strategy and simulation research of water-cooled PEMFC thermal management system[J]. CIESC Journal, 2020, 71(5): 2139-2150. (in Chinese)

[12] Zhou Su, Xie Zhengchun, Chen Chunguang, et al. Design and energy consumption research of an integrated air supply device for multi-stack fuel cell systems[J]. Applied Energy, 2022, 324: 119704.

[13] Zhou Su, Chen Chunguang, Fan Lei. Review on Thermal Management of Automotive Proton Exchange Membrane Fuel Cell Power System[J]. Automotive Digest, 2023, No.565(02):1-14. (in Chinese)

[14] Liu Yongfeng, Gao Jianhua, Pei Pucheng, et al. Effects of dynamic changes in inlet temperature on proton exchange membrane fuel cell[J]. Journal of Renewable and Sustainable Energy, 2019, 11(4): 044302.

[15] Rojas J D, Ocampo-Martínez C, Kunusch C. Thermal modelling approach and model predictive control of a water-cooled PEM fuel cell system[C]. IECON 2013-39th Annual Conference of the IEEE Industrial Electronics Society. IEEE, 2013: 3806-3811.

[16] Jin Wen, Li Zhaojia, Wei Luosi, et al. The improvements of BP neural network learning algorithm[C]. WCC 2000-ICSP 2000. 2000 5th international conference on signal processing proceedings. 16th world computer congress 2000. IEEE, 2000, 3: 1647-1649.

[17] Chen Minghao, Xu Zuhua, Zhao Jun, et al. Dynamic Matrix Control with Feed-Forward for Target Tracking[C]. 2019 12th Asian Control Conference (ASCC). IEEE, 2019: 1295-1300.